ELSEVIER

Journal of Power Sources 68 (1997) 629–633

JOURNAL OF POWER SOURCES

Cycling performance of novel lithium insertion electrode materials based on the Li–Ni–Mn–O system

Michael E. Spahr [a,b], Petr Novák [a,*], Otto Haas [a], Reinhard Nesper [b]

[a] *Paul Scherrer Institute, Electrochemistry Section, 5232 Villigen PSI, Switzerland*

[b] *Swiss Federal Institute of Technology (ETH), Laboratory of Inorganic Chemistry, ETH-Zentrum, 8092 Zurich, Switzerland*

Accepted 13 November 1996

Abstract

The electrochemical behavior of lithium–nickel–manganese mixed oxides $LiNi_{1-y}Mn_yO_{2+\delta}$ with the layered-type, rhombohedral α-$NaFeO_2$ structure ($R\bar{3}m$) prepared by means of a new solution technique has been correlated to their manganese content. Test electrodes were developed and their porosity was tuned by using either graphite or carbon black as an electronically conductive additive. The amount of carbon was optimized to achieve the maximum specific charge referred to the oxide fraction of the electrode mass. Porosities of $<20\%$ were measured for graphite-based electrodes, with median pore diameters between 0.1 and 0.01 μm. In the case of the carbon black-based electrodes, larger pore sizes and porosities of $>40\%$ were obtained for relatively small preparation pressures, leading to better wetting properties of the electrode and maximum specific charges of about 170 mAh g^{-1} (referred to the oxide) for materials with the best insertion performances, in contrast to about 150 mAh g^{-1} for oxide/graphite electrodes. A slightly better stability during cycling was observed for graphite-based electrodes which were therefore used for comparative studies. The specific charge and cycling stability of the solution-prepared pure lithium nickel oxide $LiNiO_2$ was low but was significantly enhanced by replacing some nickel with manganese. With increasing manganese content, the specific charge increased to about 160 mAh g^{-1} for materials with an Ni:Mn ratio of about 1:1. It decreased gradually during cycling to about 80 mAh g^{-1} after 50 cycles. © 1997 Elsevier Science S.A.

Keywords: Nickel manganese oxides; Lithium; Intercalation, Electrodes; Porosity, Lithium batteries

1. Introduction

The broad use of carbon as the negative electrode material in rechargeable lithium ion-transfer battery systems has generated a great demand for lithium-containing positive materials with high specific charge and cycling stability. Recently, attention has been focused on $LiNiO_2$ [1–3] which is a representative of the group of lithium-containing transition metal oxides with the layered α-$NaFeO_2$-type structure ($R\bar{3}m$) [4].

Solid-state synthesis of $LiNiO_2$ can lead to phase compositions within a phase width $0<x<0.4$ in $Li_{1-x}Ni_{1+x}O_2$, strongly depending on the synthesis conditions. Temperatures above 600 °C are necessary to complete the oxidation from Ni^{2+} to Ni^{3+} in oxygen atmosphere as well as to obtain a sufficiently high degree of crystallinity. Unfortunately, due to the volatility of Li_2O at elevated temperatures, a loss in the lithium content results [5]. The lithium-deficient stoichiometries $Li_{1-x}Ni_{1+x}O_2$ have a partially disordered cationic distribution. This defect structure is regarded as a reason for the decreased specific charge and the unstable cycling behavior of the lithium-deficient compounds [6–9].

Recently, we have reported a new solution technique in which the oxidation step from Ni^{2+} to Ni^{3+} is performed in an aqueous medium using LiOCl or LiOBr as the oxidizing agents [10]. The Ni(III) oxide hydroxide precursor, which is precipitated under the synthesis conditions, is subsequently calcined with excess of LiOH. Different amounts of manganese can be added homogeneously in a co-precipitation step to give Li–Ni–Mn mixed oxides after calcination. The oxides have shown different electrochemical insertion properties than the $LiNiO_2$ analogue synthesized via the classical solid-state synthesis route.

In this work we first developed test electrodes, whereby we optimized the electrode composition by varying the nature and amount of the carbon additive used. Then, various manganese-doped lithium nickel oxides were tested for their electrochemical performance as a function of the manganese content, y.

* Corresponding author

PII S0378-7753(96)02593-1

2. Experimental

Various $LiNi_{1-y}Mn_yO_{2+\delta}$ samples with manganese contents $0 \leq y \leq 0.5$ were prepared by adding an aqueous solution of the appropriate divalent metal nitrates to an aqueous Br_2/LiOH solution at 0 °C. The co-precipitated Ni^{3+} and Mn^{4+} oxyhydroxides were filtered, washed thoroughly with water, and mixed with 1.2 equivalents of lithium hydroxide. The following calcination was performed in a stream of oxygen at 700 °C for 10 h. The excess of Li_2O was removed from the crude products by water extraction.

A detailed characterization of the recovered materials is described elsewhere [10b]. The α-$NaFeO_2$-type structure of quaternary Li–Ni–Mn–O phase system can be maintained with up to 60 mol% manganese [11]. Our powder X-ray diffraction (XRD) experiments of the obtained $LiNi_{1-y}Mn_yO_{2+\delta}$ compounds confirmed crystalline products in which the layered $LiNiO_2$ structure was maintained for all the prepared compositions. Chemical analysis by atomic absorption/emission spectroscopy (AAS/AES), magnetic susceptibility measurements, and X-ray photoelectron spectroscopy (XPS) determined nickel and manganese to be both in the trivalent state pointing to a change of the manganese oxidation state during the calcination process at 700 °C. Table 1 relates the nominal manganese content, y, as used in the co-precipitation reaction with the analyzed stoichiometry of the recovered materials and the abbreviations for the compounds used throughout the text.

Electrodes with 1.3 cm^2 geometrical area were prepared from these oxides, different amounts of either graphite (TIMREX SFG 6, Timcal, Switzerland) or carbon black (VULCAN XC72, Cabot Europe, France, graphitized at 2700 °C for 1 h under an inert gas atmosphere), and 2 wt.% of polyisobutene binder (OPPANOL® B200, BASF, Germany). The mixture of oxide and carbon was ball-milled in a hexane solution of the binder for 4 h. The resulting slurry was dried at 80 °C and then pulverized in a laboratory mill. Finally, about 40–50 mg of the oxide/carbon/binder blend were pressed on a titanium current collector.

Slow cyclic voltammetry and galvanostatic cycling experiments were carried out in gas-tight laboratory cells with a three-electrode arrangement in which working and counter electrodes were mechanically pressed against a glass fiber separator soaked with the electrolyte consisting of 1.0 M $LiClO_4$ in propylene carbonate (PC). Metallic lithium served as the counter and reference electrodes.

The porosity and pore size distribution of the prepared electrodes were calculated from intrusion curves measured with a mercury porosimeter (Micromeritics Pore Sizer 9320).

Table 1
Manganese content, y, used in the co-precipitation reaction, analyzed stoichiometry of the recovered materials, and corresponding abbreviations as used in the text

Manganese content, y (nominal)	Stoichiometry (analyzed)	Abbreviation
0	$Li_{1.06}Ni_{1.02.03}$	Ni10Mn0
0.2	$Li_{1.17}Ni_{0.80}Mn_{0.19}O_{2.07}$	Ni8Mn2
0.4	$Li_{1.07}Ni_{0.60}Mn_{0.37}O_{1.99}$	Ni6Mn4
0.5	$Li_{1.04}Ni_{0.52}Mn_{0.48}O_{2.02}$	Ni5Mn5

3. Results and discussion

3.1. Porosity versus electrode performance

A reliable comparison of the insertion properties of the prepared oxides required the development of reproducible test electrodes. Therefore, we optimized the preparation procedure and the oxide:carbon ratio in the electrode composition to get a maximum specific charge (here always referred to the oxide fraction of the total electrode mass).

The highest specific charges were obtained with either 32 wt.% graphite or 50 wt.% graphitized carbon black. The reason that a higher amount of carbon black was necessary might be related to its lower electronic conductivity, which may decrease the overall insertion rate. In Fig. 1, the pore size distribution of electrodes having the optimal carbon content is illustrated. An absolute porosity of only 16 vol.% was attained for the electrode with 32 wt.% of graphite using a preparation pressure of 3 t cm^{-2} (which turned out to be optimal for the graphite-based electrodes). Apparently, the pressing of graphite orients the flakes on the current collector which leads to small pore sizes and compact electrodes. The pore diameters for the graphite-based electrodes are mainly distributed in the range between 0.02 and 0.1 μm. A much higher pore volume in this pore diameter range was measured for electrodes with 50 wt.% carbon black, prepared also at 3 t cm^{-2}. Moreover, a significant fraction of pores with median diameters between 1–10 μm appeared in this case. The total porosity was measured to be 32 vol.%. For graphite anodes

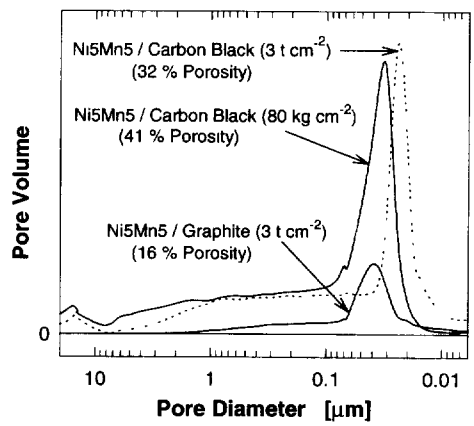

Fig. 1. Typical pore-size distribution (y-axis: arbitrary units) and porosity of the $LiNi_{1-y}Mn_yO_{2+\delta}$ electrodes consisting of 2 wt % binder and either 32 wt.% graphite or 50 wt % carbon black, using different preparation pressures.

in carbonate-based electrolytes, optimum pore sizes in the range between 1 and 10 μm were reported [12–14]. Pores in this range allow a better electrolyte-wetting of the electrode. Using lower preparation pressures, the fraction of pores with the desired diameters was even enhanced (Fig. 1). The pore diameters increased to higher values as well, i.e. the pore sizes and the absolute electrode porosity increased. For a preparation pressure of 80 kg cm^{-2}, an absolute porosity of 41 vol.% was measured for the carbon black-containing oxide electrode.

Due to the better wetting properties of the oxide/carbon black electrodes, higher specific charges are obtained. For the Ni5Mn5 oxide, 170 mAh g^{-1} were measured galvanostatically in the first charging (de-insertion) cycle to 4.3 V versus Li/Li^+ using a current density of 0.38 mA cm^{-2}. For the corresponding oxide/graphite mixture only 150 mAh g^{-1} were obtained in comparable measurement. However, the cycling experiments show better performance using graphite instead of carbon black. The oxide/graphite electrode is slightly better, as shown in Fig. 2. This behavior suggests a better mechanical stability of the oxide/graphite electrode.

These results indicate that the two electrode compositions represent the extreme cases in which either the cycling stability or the maximum specific charge is emphasized. An optimum mixture might be found in a combination of the pore-forming carbon black and the electrode stabilizing graphite. For our comparative studies of the prepared oxides we used the oxide/graphite electrode, which has the better cycling stability.

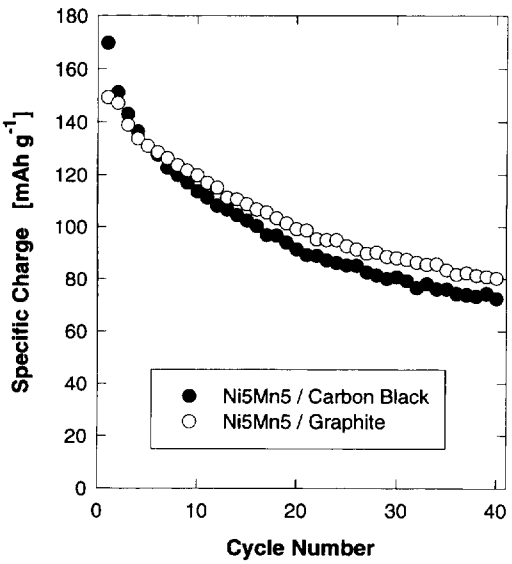

Fig. 2 Cycle dependence of the specific charge of an $LiNi_{1-y}Mn_yO_{2+\delta}$-containing electrode ($y \approx 0.5$, Ni5Mn5, Li^+ de-insertion) prepared with 32 wt.% graphite (preparation pressure of 3 t cm^{-2}) or 50 wt % carbon black (preparation pressure of 80 kg cm^{-2}), galvanostatically cycled at 0.38 mA cm^{-2}.

3.2. Oxide cycling performance

Fig. 3 demonstrates that the lithium insertion/de-insertion reaction is reversible for all tested manganese contents, y, in $LiNi_{1-y}Mn_yO_{2+\delta}$. In these potentiodynamic experiments, a maximum specific charge for Li^+ de-insertion of about 160 mAh g^{-1} was obtained for a manganese content of $y \approx 0.5$ in the potential range of 2.5–4.3 V versus Li/Li^+ in the first cycle at 50 μV s^{-1}. The specific charge of the initial cycle decreases with decreasing manganese content to about 110 mAh g^{-1} for the pure lithium nickel oxide $LiNiO_2$. We attribute the lower specific charge for $LiNiO_2$ prepared via our solution technique in comparison to the specific charge of 150–170 mAh g^{-1} [15,16] that is typically obtained for the ideal stoichiometric $LiNiO_2$ prepared via solid-state synthesis to the partial cationic disorder and lower crystallinity of the former. This fact has been confirmed by analysis of the XRD measurements and will be discussed elsewhere [10b].

Fig. 4 illustrates the cycling behavior of the mixed oxides as a function of the manganese content, y, from voltammetric experiments. Although the cycling performance of the $LiNiO_2$ (Ni10Mn0) was poor, a significant improvement was achieved with 20 mol% manganese. The specific charge and cycling stability for the oxides with 20–40 mol% manganese was comparable. A further improved performance was found for the manganese content of about 50 mol%, in which a specific charge of about 150 mAh g^{-1} was measured in the first few cycles (Fig. 4). The specific charge declines gradually from 160 to about 80 mAh g^{-1} after 50 cycles. The corresponding voltammograms are shown in Fig. 5. The height of the de-insertion peak between 3.6 and 4.0 V versus Li/Li^+ decreases during cycling, whereas an additional broad peak emerges with increasing cycle number in the potential range between 3.0 and 3.6 V versus Li/Li^+. Ex situ XRD experiments of the cycled electrode material show a dramatic decrease in diffraction peak intensity after 50 cycles. This indicates a gradual structural change of the oxide to the amorphous state during cycling.

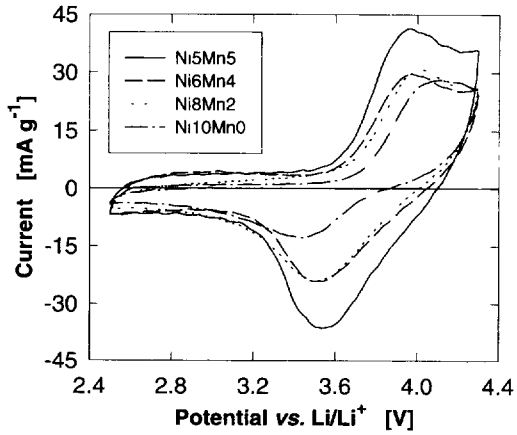

Fig. 3. Cyclic voltammograms (first cycles) of $LiNi_{1-y}Mn_yO_{2+\delta}$ with different manganese contents, y, at 50 μV s^{-1}; graphite-based electrode.

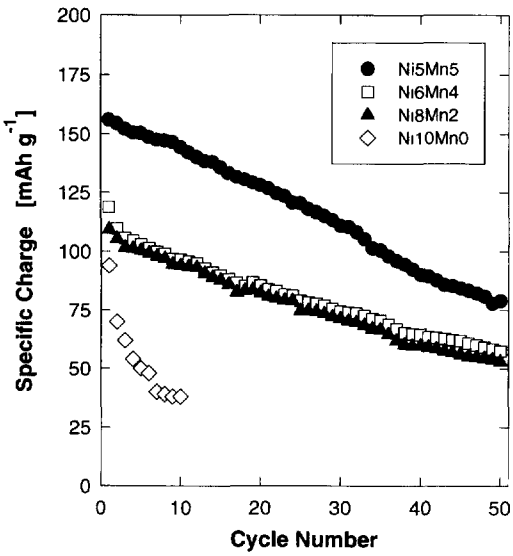

Fig 4. Specific charges for Li^+ de-insertion obtained from cyclic voltammetry (as in Fig 3) of the $LiNi_{1-y}Mn_yO_{2+\delta}$ with different manganese contents, y; graphite-based electrode.

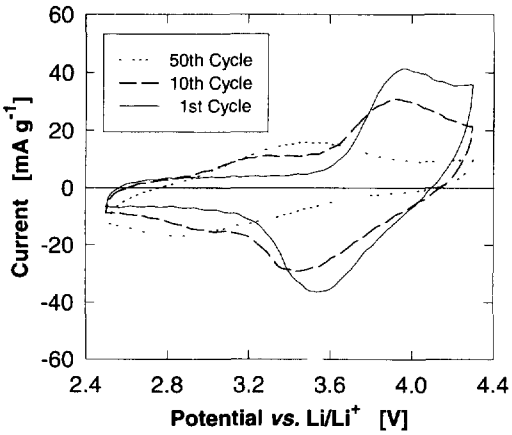

Fig 5. Cyclic voltammograms of Ni5Mn5 (graphite-based electrode) at 50 $\mu V\ s^{-1}$

For manganese contents of more than 50 mol%, spinel-type materials were obtained. The amount of Li^+ which de-inserted from these materials in the first discharge is much less than for the layered-type mixed oxides. However, these spinels show attractive specific charges for a reversible Li^+ insertion in the 3 V region. The results for these spinel-type oxides will be described in a forthcoming paper.

4. Conclusions

Mixed lithium–nickel–manganese oxide was synthesized via a novel solution technique in which a mixed transition metal hydroxide precursor was prepared in an oxidative co-precipitation process prior to a calcination step. We have shown the importance of electrode porosity and carbon content for the performance of $LiNi_{1-y}Mn_yO_{2+\delta}$ in test electrodes. Higher porosity of oxide/carbon black electrode leads to faster electrode kinetics which is reflected in higher specific charges and sharper voltammetric peaks. However, on long-term cycling, the higher mechanical stability of oxide/graphite electrodes leads to better results.

In view of the electrochemical performance of the series of $LiNi_{1-y}Mn_yO_{2+\delta}$ oxides, increasing specific charges and improved cycling performance was found for an increasing manganese content up to $y \approx 0.5$. Although the specific charge obtained for the $LiNiO_2$ is rather low, about 170 mAh g^{-1} was achieved for the Ni:Mn ratio of about 1:1. This is in contrast with the $LiNiO_2$ synthesized either via the classical solid-state route or via the 'chimie douce' route, for which manganese doping has led to a deterioration of the electrochemical performance [11,17,18]. About 150 mAh g^{-1} was measured in the initial cycles for the oxide with the nominal composition $LiNi_{0.5}Mn_{0.5}O_2$ (Ni5Mn5). The specific charge gradually decreased to about 80 mAh g^{-1} after 50 cycles.

Acknowledgements

This work is part of a project partially financed by the Swiss Federal Office of Energy which is devoted to the development of graphite and oxide electrodes for lithium ion-transfer batteries. We thank Dr B. Schnyder, PSI for the XPS measurements.

References

[1] T. Ohzuku, in G. Pistoia (ed.), *Lithium Batteries*, Elsevier, Amsterdam, 1994, Ch. 6
[2] T. Ohzuku, A. Ueda, M. Nagayama, Y. Iwakoshi and H. Komori, *Electrochim. Acta, 38* (1993) 1159.
[3] J.R. Dahn, U. von Sacken, M.W. Juzkow and H. Al-Janaby, *J. Electrochem. Soc., 138* (1991) 2207.
[4] (a) L.D. Dyer, B.S. Borie and G.P. Smith, *J. Am. Chem. Soc., 76* (1954) 1499; (b) J.B. Goodenough, D.G. Wickham and W.J. Croft, *J. Phys. Chem. Solids, 5* (1958) 107.
[5] R. Kanno, H. Kubo, Y. Kawamoto, T. Kamiyama, F. Izumi, Y. Takeda and M. Takano, *J. Solid State Chem., 110* (1994) 216
[6] J. Morales, C. Perez-Vicente and J.L. Tirado, *Mater. Res. Bull., 25* (1990) 623.
[7] W. Li, J.N. Reimers and J.R. Dahn, *Phys. Rev., B46* (1992) 3236
[8] T. Ohzuku, H. Komori, M. Nagayama, K. Sawai and T. Hirai, *Chem. Express, 6* (1991) 161.
[9] J.R. Dahn, U. von Sacken and C.A. Michal, *Solid State Ionics, 44* (1990) 87
[10] (a) M.E. Spahr, P. Novák, O. Haas and R. Nesper, *Chimia, 49* (1995) 283, (b) M.E. Spahr, P. Novák, B. Schnyder, O. Haas and R. Nesper, *J. Electrochem. Soc.*, (1997) submitted for publication
[11] E. Rossen, C.D.W. Jones and J.R. Dahn, *Solid State Ionics, 57* (1992) 311

[12] V. Manev, I. Naidenov, B Puresheva, P. Zlatilova and G. Pistoia, *J. Power Sources, 57* (1995) 133.
[13] V Manev, I. Naidenov, B. Puresheva, P. Zlatilova and G. Pistoia, *J. Power Sources, 55* (1995) 211.
[14] P. Novák, W. Scheifele, M. Winter and O. Haas, *J. Power Sources, 68* (1997) 267–270.
[15] W Ebner, D. Fouchard and L. Xie, *Solid State Ionics, 69* (1994) 238
[16] M. Broussely, F. Perton, P. Biensan, J.M. Bodet, J. Labat, A. Lecerf, C. Delmas, A Rougier and J P. Pérès, *J. Power Sources, 54* (1995) 109.
[17] Y. Nitta, K. Okamura, K Haraguchi, S. Kobayashi and A Ohta, *J Power Sources, 54* (1995) 511
[18] D. Caurant, N. Baffier, V Bianchi, G. Grégoire and S Bach, *J. Mater. Chem., 6* (1996) 1149.